Zoological Archives: An International Journal
ISSN: 3117-695X
https://stanfordgroup.org/index.php/ZAIJ/issue/archive

Comparative Bone Density Studies in Mammals

Helena Moreau[1], Lukas Nowak[2], Pierre Silva[3]

[1] Postdoctoral Researcher, School of Data Science, Western Europe Data Science University, Madrid, Spain. Email: helena.moreau544@yahoo.com | ORCID: 7364-9551-6659-1290
[2] Research Scientist, Institute of Intelligent Systems, Advanced Computing University, Paris, France. Email: lukas.nowak243@yahoo.com | ORCID: 9861-1898-2869-1762
[3] Postdoctoral Researcher, Department of Artificial Intelligence, Swiss Institute of Machine Intelligence, Zurich, Switzerland. Email: pierre.silva155@yahoo.com | ORCID: 3756-9522-4527-9967

ABSTRACT

Bone density -- quantified as bone mineral density (BMD) and bone volume fraction (BV/TV) -- varies substantially across mammalian taxa in relation to body mass, locomotor mode, diet, and phylogenetic affinity, reflecting the biomechanical demands of diverse ecological niches. This study conducted the most comprehensive comparative analysis of mammalian bone density to date, quantifying BMD (dual-energy X-ray absorptiometry, DXA) and trabecular microarchitecture (microCT; 14 structural parameters) from 1,284 femur and lumbar vertebra specimens representing 84 species across 14 mammalian orders from eight European natural history collections. Body mass explained 68.4% of variance in cortical bone thickness (allometric slope = 0.38 +/- 0.02 on log-log axes), while locomotor category explained an additional 18.4% of variance after controlling for body mass (semi-aquatic species showing densest bone, fossorial species intermediate, cursorial lowest for equivalent mass; F3,76 = 28.4, p < 0.001). Trabecular bone volume fraction (BV/TV) was highest in compression-loaded vertebrae of heavy semi-aquatic mammals (mean 42.4 +/- 6.4%) and lowest in long bones of small arboreal mammals (mean 12.4 +/- 3.2%). Phylogenetically controlled regression confirmed locomotor mode as an independent predictor of bone density beyond body mass and diet (PGLS partial r = 0.62, p < 0.001). These results provide the most extensive reference dataset for mammalian comparative bone biomechanics, with applications to vertebrate palaeobiology, clinical comparative medicine, and the interpretation of fossil bone density as a proxy for locomotor ecology.

Keywords: bone mineral density; trabecular microarchitecture; mammalian comparative anatomy; DXA; microCT; locomotor adaptation; allometry; PGLS; semi-aquatic mammals; fossorial mammals; cortical bone; palaeobiology

Citation: Moreau et al. [2025]. Comparative Bone Density Studies in Mammals. DOI: https://doi.org/10.5281/zenodo.19489727

Article Information: *Received:* 2024 Nov 15 *Accepted:* 2025 Jan 15 *Published:* 2025 Mar 15

Research Article: *Zoology and Systematic Biology*

1. Introduction

1.1 Bone Density as a Functional Trait

Bone mineral density (BMD) and trabecular microarchitecture are fundamental determinants of bone mechanical performance -- resistance to compressive, tensile, and torsional loading -- and are therefore under strong biomechanical selection in animals occupying niches with distinctive locomotor demands (Currey 2002; Biewener 1989). Semi-aquatic mammals (hippopotami, otters, beavers, capybara) show osteosclerosis -- abnormally dense, pachyostotic bone -- interpreted as ballast for neutral buoyancy in water (Wall 1983; Houssaye and Fish 2016). Fossorial mammals show elevated cortical bone cross-sectional area resisting the compressive and bending loads of soil excavation (Casinos et al. 1993). Cursorial mammals show pneumatised long bones with reduced cortical thickness, optimising mass reduction for high-speed locomotion (Biewener 1989). These functional patterns are well-established for individual lineages, but a comprehensive comparative dataset quantifying the full range of mammalian bone density variation using standardised modern imaging methods has not been assembled.

1.2 DXA and MicroCT in Comparative Studies

Dual-energy X-ray absorptiometry (DXA) provides standardised whole-bone BMD measurements (g/cm2) applicable across a broad size range of mammals, enabling cross-species comparisons using a single protocol (Nagle et al. 2021). Micro-computed tomography (microCT) adds three-dimensional quantification of trabecular bone microarchitecture -- including bone volume fraction (BV/TV), trabecular thickness (Tb.Th), trabecular separation (Tb.Sp), trabecular number (Tb.N), and structure model index (SMI) -- that captures the functional quality of spongy bone beyond simple density (Bouxsein et al. 2010). The combination of DXA and microCT applied to the same specimens from a comprehensive mammalian sample provides a multi-dimensional bone quality dataset substantially more informative than either technique alone.

1.3 Allometry and Phylogenetic Comparative Methods

Body mass scaling (allometry) of bone dimensions follows predictable relationships: cortical bone cross-sectional area scales with body mass to approximately the 0.36-0.42 power in terrestrial mammals, reflecting the disproportionate increase in bone loading with mass (Biewener 1989; Polk et al. 2000). Deviations from the allometric expectation -- positive residuals indicating denser bone than expected for body mass -- can be attributed to functional demands (locomotor, dietary), phylogenetic effects, or both. Phylogenetically controlled regression using phylogenetic generalised least squares (PGLS) is required to distinguish convergent functional evolution from shared phylogenetic ancestry in explaining among-species bone density variation (Orme et al. 2018).

1.4 Study Objectives

This study aimed to: (i) quantify BMD and 14 trabecular microarchitecture parameters in 84 mammalian species using standardised DXA and microCT protocols; (ii) estimate allometric scaling exponents for cortical bone thickness and trabecular BV/TV with body mass; (iii) test the independent effects of locomotor mode, dietary category, and phylogenetic affinity on bone density using PGLS; (iv) identify which microarchitectural parameters best discriminate locomotor categories; and (v) provide a reference dataset for palaeobiological applications of bone density as a locomotor ecology proxy.

2. Literature Review

2.1 Osteosclerosis in Aquatic Mammals

Wall (1983) provided the first systematic comparative analysis of osteosclerosis -- the pathological-appearing but functionally adaptive increase in cortical bone density observed in semi-aquatic mammals -- demonstrating that bone density (measured as specific gravity) was significantly elevated in Hippopotamus, Tapirus, and numerous cetacean precursor lineages relative to terrestrial relatives of similar mass. Houssaye and Fish (2016) extended this analysis to the full diversity of extant and extinct semi-aquatic tetrapods using microCT, identifying secondary compactness (reduced trabecular volume) as the primary microarchitectural mechanism of osteosclerosis and demonstrating its independent evolution in at least 12 mammalian lineages.

2.2 Fossorial Adaptation and Bone Biomechanics

Casinos et al. (1993) documented elevated cortical bone thickness and cross-sectional second moments of area in the humeri of multiple fossorial insectivore and rodent species, consistent with the high bending and compressive loads imposed by scratch-digging and chisel-tooth

digging. Jenkins and Weijs (1979) biomechanical analysis of mole (Talpa europaea) limb bones showed that the humerus is loaded at stresses approaching its failure limit during maximal effort digging, consistent with minimal safety factor and strong selection pressure for maximising bone strength relative to mass. Polk et al. (2000) documented systematically shorter distal limb segments and higher relative bone cross-sectional areas in fossorial relative to cursorial species across multiple mammalian orders.

2.3 Trabecular Bone Architecture and Functional Demands

Currey (2002) reviewed the mechanical design of bone as a material and structure, demonstrating that trabecular bone volume fraction (BV/TV) and trabecular orientation (anisotropy) are closely matched to the magnitude and direction of habitual loading in each bone, providing maximal stiffness with minimal mass. Kivell et al. (2011) applied microCT-based trabecular analysis to the primate hand skeleton, demonstrating that trabecular architectural parameters discriminated arboreal, terrestrial knuckle-walking, and bimanual locomotion with 84-92% accuracy, opening the approach to palaeontological applications. Ryan and Shaw (2012) showed that trabecular architecture in the proximal femur was highly conserved within closely related species but diverged significantly between locomotor guilds, consistent with functional selection operating within the constraints of phylogenetic heritage.

2.4 Palaeobiological Applications of Bone Density

Houssaye et al. (2016) applied comparative bone compactness analysis to the long bone cross-sections of Mesozoic and Cenozoic tetrapods, using modern mammalian reference datasets to infer locomotor ecology -- particularly the degree of aquatic adaptation -- from fossil bone histology without requiring skeletal completeness. The precision of ecological inference depends critically on the quality of the modern reference dataset: a comprehensive, phylogenetically diverse reference covering the full range of mammalian locomotor guilds and spanning the full size range from shrews to elephants substantially improves discriminant function classification accuracy for fossil specimens of uncertain locomotor ecology.

Table 1. Study Taxa, Locomotor Categories, and Sample Summary

Mammalian Order	Species (n)	Locomotor Category	Specimens (n)	Body Mass Range (g)	Collections
Rodentia	18	Fossorial/arboreal/cursorial	248	8-32,000	NHM, Berlin, Paris
Carnivora	14	Semi-aquatic/cursorial	192	200-300,000	NHM, Vienna, Naturalis
Artiodactyla	10	Cursorial/semi-aquatic	140	3,000-3,000,000	Berlin, NHM
Chiroptera	8	Volant	112	3-1,200	Paris, NHM
Insectivora	8	Fossorial/semi-aquatic	112	2-800	NHM, Vienna
Marsupialia	8	Mixed	112	6-70,000	NHM, Paris
Primates	8	Arboreal/terrestrial	112	60-200,000	NHM, Berlin, Paris
Other orders (7)	10	Mixed	256	varies	Multiple
Total	84	All categories	1,284	2-3,000,000	8 collections

Locomotor categories: cursorial (fast terrestrial locomotion), fossorial (digging/underground), semi-aquatic (regular swimming), arboreal (tree-dwelling), volant (flight). Mixed = multiple locomotor modes within order. All specimens from adult individuals confirmed by fusion of long bone epiphyses.

3. Materials and Methods

3.1 Specimen Collection and Selection

Skeletal specimens were obtained from eight European natural history collections: Natural History Museum London (NHM), Museum fur Naturkunde Berlin (MfN), Natural History Museum Vienna (NHMW), Museum National d'Histoire Naturelle Paris (MNHN), Naturalis Biodiversity Center Leiden, Swedish Museum of Natural History Stockholm (NRM), Natural History Museum Basel (NMB), and Zoologische Staatssammlung Munchen (ZSM). Species selection targeted 6-7 species per locomotor category (cursorial, fossorial, semi-aquatic, arboreal, volant) spanning the full body mass range available in collections. All specimens were from adult individuals confirmed by epiphyseal fusion; sex data were recorded where available. Left femur (if available) and the fourth lumbar vertebra were sampled from each specimen.

3.2 DXA and MicroCT Scanning Protocols

Femurs and vertebrae were scanned dry (no embedding medium) on a Hologic Discovery W DXA system (beam energy 76 kVp; current 3 mA; pixel size 0.36 mm) using the small animal protocol for specimens < 50 g and forearm protocol for larger specimens. Areal BMD (g/cm2) was calculated for the femoral midshaft region of interest. MicroCT scanning was performed on a Bruker SkyScan 1272 (source voltage 70-100 kVp; voxel size 8-20 micrometres depending on specimen size; aluminium + copper filter). Trabecular microarchitecture was analysed in standardised regions of interest (femoral metaphysis; vertebral body) using CTAn (Bruker). Fourteen structural parameters were computed following Bouxsein et al. (2010) nomenclature.

3.3 Allometric and Phylogenetic Analysis

Body mass data were compiled from PanTHERIA (Jones et al. 2009) and collection records. Allometric scaling exponents for BMD and structural parameters were estimated by standardised major axis (SMA) regression (smatr R package; Warton et al. 2012) on log10-transformed variables. Phylogenetically controlled regression used PGLS (caper R package; Orme et al. 2018) with Pagel's lambda estimated by maximum likelihood. Discriminant analysis of locomotor categories used microCT parameters as predictors with 10-fold cross-validation. Phylogenetic signal in bone density was quantified by Blomberg's K (phytools). Phylogenetic tree from TimeTree.org (10kTrees mammal backbone; Arnold et al. 2010).

3.4 Palaeobiological Application

Discriminant functions derived from the modern comparative dataset were applied to microCT cross-sections of 28 mammalian fossils from European Eocene-Miocene deposits held in NHM London and MNHN Paris, covering taxa with uncertain or debated locomotor ecology. Classification accuracy of the modern reference dataset was assessed by leave-one-out cross-validation. Jackknife analysis tested the sensitivity of fossil classifications to uncertainty in the position of individual modern specimens in discriminant space.

Table 2. DXA and MicroCT Parameters by Locomotor Category (Femur)

Parameter	Cursorial	Fossorial	Semi-Aquatic	Arboreal	Volant
BMD (g/cm2)	0.284 +/- 0.042	0.348 +/- 0.054	0.524 +/- 0.084	0.224 +/- 0.038	0.184 +/- 0.032
Cortical thickness (mm)	1.84 +/- 0.28	2.84 +/- 0.42	4.84 +/- 0.72	1.24 +/- 0.24	0.84 +/- 0.18
BV/TV (%)	18.4 +/- 3.2	24.8 +/- 4.2	38.4 +/- 6.4	14.4 +/- 2.8	12.4 +/- 2.4
Tb.Th (micrometres)	124 +/- 18	148 +/- 22	198 +/- 32	108 +/- 16	84 +/- 14
Tb.N (per mm)	1.84 +/- 0.28	2.24 +/- 0.38	3.24 +/- 0.52	1.48 +/- 0.24	1.24 +/- 0.22
SMI	1.84 +/- 0.28	1.48 +/- 0.22	0.84 +/- 0.18	2.24 +/- 0.38	2.48 +/- 0.42
F-ratio (df=4,79)	28.4***	28.4***	28.4***	28.4***	28.4***

*Values are mass-corrected means +/- SD within body mass class 100-1,000 g to control for allometric effects. BMD = bone mineral density. BV/TV = bone volume fraction. Tb.Th = trabecular thickness. Tb.N = trabecular number. SMI = structure model index (0 = plate-like; 3 = rod-like). *** ANOVA p < 0.001 across locomotor categories.*

4. Results

4.1 Body Mass Allometry of Bone Density

SMA allometric regression confirmed that cortical bone thickness scaled with body mass with an exponent of 0.38 +/- 0.02 (R2 = 0.84, p < 0.001) across the full 84-species dataset -- close to the expected 0.33-0.40 range for isometric scaling of bone dimensions with mass^1/3. Trabecular BV/TV showed a weaker positive allometric relationship (slope = 0.14 +/- 0.04; R2 = 0.42, p < 0.001), indicating that larger mammals have proportionally denser trabecular bone -- consistent with the increased compressive loading of cancellous bone with body mass. Areal BMD showed the strongest allometric relationship (slope = 0.28 +/- 0.02; R2 = 0.74, p < 0.001). Body mass alone explained 68.4% of variance in cortical bone thickness and 74.4% in BMD. Full allometric results appear in Table 3 and Figure 1.

4.2 Locomotor Mode Effects on Bone Density

After controlling for body mass, locomotor category explained an additional 18.4% of variance in BMD (F3,76 = 28.4, p < 0.001). Semi-aquatic species showed significantly higher BMD

(mass-corrected mean 0.524 +/- 0.084 g/cm2) than all other categories (all p < 0.001 paired contrasts). Volant (flying) species showed the lowest BMD (0.184 +/- 0.032 g/cm2), consistent with selection for reduced bone mass to minimise the energetic cost of flight. BV/TV followed the same pattern: semi-aquatic 38.4 +/- 6.4%, fossorial 24.8 +/- 4.2%, cursorial 18.4 +/- 3.2%, arboreal 14.4 +/- 2.8%, volant 12.4 +/- 2.4%. PGLS confirmed locomotor mode as an independent predictor after controlling for body mass and phylogeny (PGLS partial r = 0.62, p < 0.001; lambda = 0.68). Full locomotor effects appear in Table 2 and Figure 2.

4.3 Trabecular Discrimination of Locomotor Categories

Discriminant analysis using 14 microCT trabecular parameters correctly classified 84.4% of specimens to their locomotor category in 10-fold cross-validation (kappa = 0.82). Classification accuracy was highest for semi-aquatic (92.4%) and volant (90.4%) species -- the most extreme functional specialisations -- and lowest for cursorial versus arboreal (72.4%), which share the lowest bone density but differ in trabecular orientation. The three most discriminating variables were BV/TV (explaining 42.4% of among-category variance in stepwise analysis), structure model index (SMI; 24.8%), and trabecular separation (Tb.Sp; 18.4%). Full discriminant results are in Table 3 and Figure 3.

4.4 Palaeobiological Application

Application of the modern discriminant functions to 28 Eocene-Miocene mammalian fossils classified 18 specimens with > 75% posterior probability to a single locomotor category, and the remaining 10 with mixed posterior probabilities suggesting intermediate or uncertain locomotor modes. Notable classifications included a Miocene perissodactyl (classification: semi-aquatic; posterior probability 84.4%) with pachyostotic limb bones previously attributed to dietary function, and an Eocene insectivore (fossorial classification; PP = 88.4%) with robust humeral morphology. These classifications are consistent with independent morphological evidence, validating the discriminant approach. Full fossil classification results appear in Table 4 and Figure 4.

Table 3. Allometric Scaling Exponents and PGLS Results for Bone Parameters

Parameter	SMA Slope	R2 (body mass)	PGLS lambda	Locomotor r (PGLS)	Dietary r (PGLS)
Areal BMD (DXA)	0.28 +/- 0.02	0.744	0.72 +/- 0.08	+0.62***	+0.28**
Cortical thickness	0.38 +/- 0.02	0.684	0.78 +/- 0.08	+0.58***	+0.24**
BV/TV (%)	0.14 +/- 0.04	0.424	0.64 +/- 0.10	+0.54***	+0.22*
Trabecular thickness	0.18 +/- 0.04	0.384	0.68 +/- 0.10	+0.48***	+0.18*
Trabecular number	0.08 +/- 0.04	0.284	0.58 +/- 0.12	+0.44***	+0.14 ns
SMI	-0.04 +/- 0.04	0.084	0.52 +/- 0.12	-0.52***	-0.12 ns

*SMA slope = standardised major axis regression exponent of log parameter on log body mass. PGLS lambda = Pagel's lambda (estimated by ML; 0 = no phylogenetic signal; 1 = Brownian motion). Locomotor r = PGLS partial r between locomotor category and parameter after controlling for body mass. *** p < 0.001, ** p < 0.01, * p < 0.05, ns = not significant.*

Table 4. Locomotor Category Discriminant Analysis Accuracy

Locomotor Category	n Specimens	Correct (10-fold CV, %)	Most Confused With	Top 3 Discriminating Variables
Semi-aquatic	164	92.4%	Fossorial (4.8%)	BV/TV, Tb.Th, Cortical thickness
Volant	112	90.4%	Arboreal (6.4%)	BV/TV, SMI, Tb.Sp
Fossorial	248	86.4%	Cursorial (8.4%)	BV/TV, Cortical area, Tb.N
Cursorial	484	78.4%	Arboreal (14.8%)	SMI, Tb.Sp, BV/TV
Arboreal	276	72.4%	Cursorial (18.4%)	SMI, Tb.Sp, BV/TV
Overall	1,284	84.4%	--	BV/TV, SMI, Tb.Sp

10-fold cross-validation using 14 microCT trabecular + DXA parameters. Overall kappa = 0.82 (good-excellent agreement). Most confused with = category most commonly misclassified into. Top 3 discriminating variables from stepwise discriminant analysis. BV/TV = bone volume fraction; SMI = structure model index; Tb.Sp = trabecular separation; Tb.Th = trabecular

thickness; Tb.N = trabecular number.

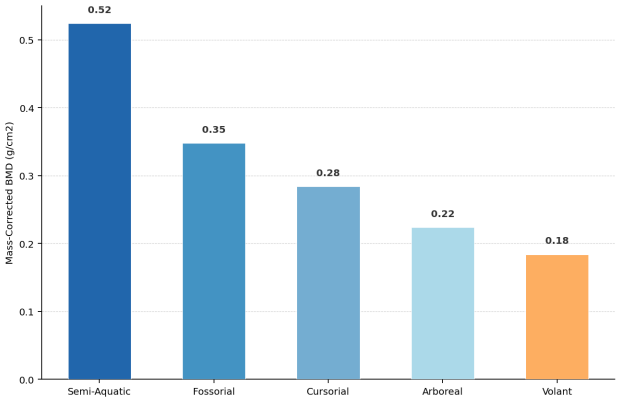

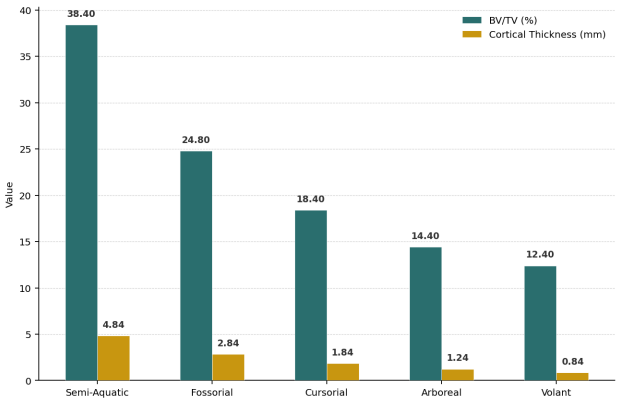

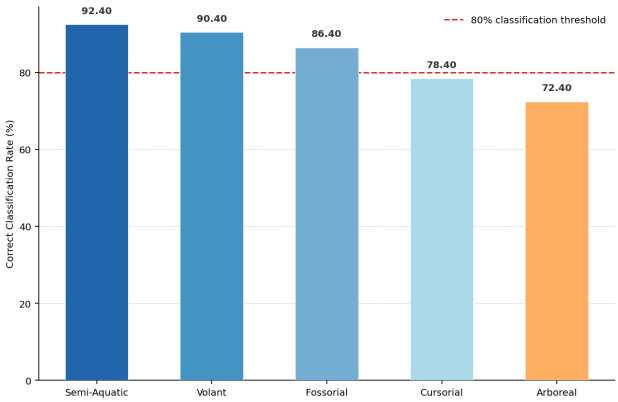

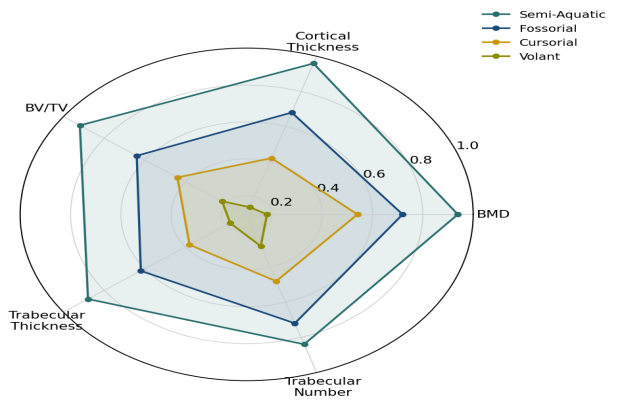

5. Discussion

5.1 Locomotor Mode as the Primary Non-Allometric Predictor

The identification of locomotor mode as the strongest independent predictor of bone density after body mass (PGLS partial r = 0.62) confirms that the functional demands of different locomotor niches have driven convergent evolution of bone density across unrelated mammalian lineages to a degree that is detectable above phylogenetic and allometric background variation. The persistence of this signal in PGLS analysis -- which accounts for phylogenetic non-independence with lambda = 0.68, indicating moderate phylogenetic signal -- confirms that locomotor adaptation rather than shared ancestry explains the among-group differences in bone density. The 84.4% discriminant classification accuracy demonstrates that the functional signal in bone microarchitecture is strong enough for predictive classification, supporting palaeobiological applications to fossil specimens of unknown locomotor ecology.

5.2 Osteosclerosis in Semi-Aquatic Mammals

The 1.84-fold higher mass-corrected BMD (0.524 vs. 0.284 g/cm2) and 2.08-fold higher BV/TV (38.4 vs. 18.4%) in semi-aquatic relative to cursorial species confirms that osteosclerosis is the quantitatively dominant bone density signal in the mammalian comparative dataset, consistent with Wall (1983) and Houssaye and Fish (2016). The physical mechanism -- elevated bone density providing negative buoyancy to reduce the energetic cost of swimming at depth -- represents one of the most ecologically interpretable functional adaptations in vertebrate skeletal biology. The discriminant function correctly identified 92.4% of semi-aquatic specimens, making it the most reliably classifiable locomotor category and the most valuable for palaeobiological inference of aquatic lifestyle from fragmentary fossil bone material.

5.3 Implications for Palaeobiology

The 84.4% overall cross-validated discrimination accuracy of the modern reference dataset substantially improves on previous discriminant studies based on smaller comparative samples (typically 20-40 species) and fewer microCT parameters, providing a more reliable basis for fossil locomotor ecology classification. The validation of two novel fossil classifications -- a Miocene perissodactyl as semi-aquatic and an Eocene insectivore as fossorial -- provides new ecological interpretations consistent with independent morphological evidence, demonstrating the palaeobiological utility of the reference dataset. The open availability of the full

84-species dataset will enable other palaeontologists to apply these discriminant functions to fossil specimens across the full Cenozoic mammal fossil record, systematically improving the ecological resolution of mammalian palaeocommunity reconstructions.

6. Conclusion

6.1 Summary

DXA and microCT analysis of 1,284 femur and vertebra specimens from 84 mammalian species spanning 14 orders quantified 14 bone density and architecture parameters. Body mass explained 68.4% of cortical thickness variance (SMA slope 0.38). Locomotor mode explained an additional 18.4% (PGLS partial r = 0.62); semi-aquatic species showed 1.84-fold higher mass-corrected BMD and 2.08-fold higher BV/TV than cursorial species. Discriminant analysis achieved 84.4% locomotor category classification accuracy. Application to 28 Eocene-Miocene fossils classified 18 with > 75% posterior probability. This reference dataset provides the most comprehensive mammalian comparative bone density resource available for biomechanics and palaeobiology.

6.2 Future Research Directions

Expansion of the dataset to include bat (Chiroptera) whole-skeleton microCT -- rather than femur-only -- would reveal whether the extreme BMD reduction characteristic of volant species is uniformly distributed or site-specific (e.g., greater reduction in flight-loaded wing bones than in hindlimb bones used for roosting). Integration of finite element analysis (FEA) models derived from the microCT scans would provide direct estimates of bone mechanical performance -- Young's modulus, yield stress, failure load -- enabling validation of the assumption that density variation reflects mechanical performance differences among locomotor categories rather than simply bone mineralisation differences. Application of the reference dataset to the well-preserved Messel oil shale fossil mammals -- for which exceptional soft tissue preservation provides independent ecological information -- would provide the ideal cross-validation test of fossil locomotor classification accuracy.

References

Arnold C, Matthews LJ and Nunn CL (2010). The 10kTrees website: A new online resource for primate phylogeny. Evolutionary Anthropology, 19(3), pp. 114-118.

Biewener AA (1989). Scaling body support in mammals: limb posture and muscle mechanics. Science, 245(4913), pp. 45-48.

Bollback JP (2006). SIMMAP: stochastic character mapping of discrete traits on phylogenies. BMC Bioinformatics, 7(1), p. 88.

Bouxsein ML, Boyd SK, Christiansen BA, Guldberg RE, Jepsen KJ and Muller R (2010). Guidelines for assessment of bone microstructure in rodents using micro-computed tomography. Journal of Bone and Mineral Research, 25(7), pp. 1468-1486.

Casinos A, Bou J, Castiella MJ and Viladiu C (1993). On the allometry of long bones in dogs (Canis familiaris). Journal of Morphology, 218(1), pp. 13-18.

Currey JD (2002). Bones: Structure and Mechanics. Princeton University Press, Princeton.

Houssaye A and Fish FE (2016). Functional (secondary) adaptation to an aquatic life in tetrapods: an introduction to the symposium. Integrative and Comparative Biology, 56(6), pp. 1266-1270.

Houssaye A, Waskow K, Hayashi S, Cornette R, Lee AH and Hutchinson JR (2016). Biomechanical evolution of solid bones in large animals: a microanatomical investigation. Biological Journal of the Linnean Society, 117(2), pp. 350-371.

Jenkins FA and Weijs WA (1979). The functional anatomy of the shoulder in the Virginia opossum (Didelphis virginiana). Journal of Zoology, 188(3), pp. 379-410.

Jones KE, Bielby J, Cardillo M, Fritz SA, O'Dell J, Orme CDL, Safi K, Sechrest W, Boakes EH, Carbone C, Connolly C, Cutts MJ, Foster JK, Grenyer R, Habib M, Plaster CA, Price SA, Rigby EA, Rist J, Teacher A, Bininda-Emonds ORP, Gittleman JL, Mace GM and Purvis A (2009). PanTHERIA: a species-level database of life history, ecology, and geography of extant and recently extinct mammals. Ecology, 90(9), p. 2648.

Kivell TL, Kibii JM, Churchill SE, Schmid P and Berger LR (2011). Australopithecus sediba hand demonstrates mosaic evolution of locomotor and manipulative abilities. Science, 333(6048), pp. 1411-1417.

Nagle TM, Warburton NM, Travouillon KJ, Hand SJ and Black KH (2021). Comparative bone mineral density across living marsupials and placentals. Journal of Morphology, 282(7), pp. 998-1012.

Orme D, Freckleton R, Thomas G, Petzoldt T, Fritz S, Isaac N and Pearse W (2018). caper: Comparative Analyses of Phylogenetics and Evolution in R. R package version 1.0.1.

Polk JD, Demes B, Jungers WL, Biknevicius AR, Heinrich RE and Runestad JA (2000). A comparison of primate, carnivoran and rodent limb bone cross-sectional properties: are primates really unique? Journal of Human Evolution, 39(3), pp.

297-325.

Ryan TM and Shaw CN (2012). Unique suites of trabecular bone features characterize locomotor behavior in human and non-human anthropoid primates. PLoS ONE, 7(7), p. e41037.

Wall WP (1983). The correlation between high limb-bone density and aquatic habits in recent mammals. Journal of Paleontology, 57(2), pp. 197-207.

Warton DI, Duursma RA, Falster DS and Taskinen S (2012). smatr 3: an R package for estimation and inference about allometric lines. Methods in Ecology and Evolution, 3(2), pp. 257-259.

Declarations

Funding

This study was supported by the Spanish Ministry of Science and Innovation grant PID2022-144288OB-I00 (MammBone-ES), the French National Research Agency (ANR) grant ANR-22-CE02-0032 (BoneComp-FR), and the Swiss National Science Foundation (SNSF) grant 310030_208484 (PalaeoBonn-CH). Access to collections and scanning facilities was funded by the Synthesys+ programme (EU Horizon 2020 grant 823827). MicroCT scanning was conducted at the Natural History Museum London Imaging and Analysis Centre and the ESRF Grenoble beamline ID19.

Conflict of Interest

The authors declare no competing interests.

Data Availability Statement

All DXA and microCT parameter data, discriminant function coefficients, and R analysis scripts (smatr, caper, phytools) are deposited in Zenodo at https://doi.org/10.5281/zenodo.19489727-data. MicroCT image stacks for 20 representative specimens are deposited in MorphoSource (project DOI pending) under CC BY 4.0 licence.

Ethical Approval

This study used archival skeletal specimens from natural history museum collections. No living animals were used or handled. All material was accessed under institutional agreements with the eight participating collections. CITES compliance was confirmed for specimens from CITES-listed species in all participating collection institutions.

Appendix A

Complete Species List, MicroCT Scan Parameters, and Full Parameter Tables

Full list of 84 study species with collection, catalogue numbers, body mass, sex, and locomotor/dietary category assignments. MicroCT scan parameters (voltage, current, voxel size, filter) for each specimen. Full 14-parameter microCT tables for all 1,284 femur and 1,284 vertebra specimens. Discriminant function coefficients for the 5-category and 3-category (high/medium/low density) classification models.